ELECTRONIC SUPPLEMENTARY INFORMATION

DOI:

Title: Luminescent MOF polymer mixed matrix membranes for humidity sensing in real status analysis

Authors: Johannes M. Stangl,[a] Dennis Dietrich,[b] Alexander E. Sedykh,[a] Christoph Janiak,[b] and Klaus Müller-Buschbaum[a*]

Experimental

General:
The synthesis of the MOFs and the MMMs as well as the analytic preparations were performed under inert conditions (argon or nitrogen atmosphere) through vacuum-line, Schlenck technique and gloveboxes (MBraun, Labmaster SP and Innovative technology, Pure Lab). The MOFs were prepared in DURAN® ampoules, which were placed in heating furnaces with Al_2O_3 tubes, a Kanthal resistance heating wire, and NiCr/Ni temperature elements controlled by Eurotherm 2416 control units. Strontium and europium metals (Smart Elements, 99.99 %), barium metal (Sigma Aldrich 99.99 %) and 1*H*-imidazole (HIm, Sigma–Aldrich 99.5 %) were applied as purchased. Dichloromethane (DCM, Fisher Chemicals >99.9 %) was dried with an MBraun solvent purification system. O_2 gas (Air Liquide, 99.998 %, water content 5 ppmv) for the gas-permeation experiments was used as received. For the cold saturated salt solutions, lithium chloride, potassium acetate (both Grüssing, 99%), potassium carbonate (Fisher Scientific, 99.94%), magnesium nitrate (Fluka, >99%) and sodium chloride (KB, 99.5%) were used as delivered.

Powder X-Ray Diffraction (PXRD) analysis was carried out on a Bruker D8 Discover diffractometer with Da Vinci design and linear Lynx-Eye detector. The X-radiation (Cu-Kα_1; λ = 154.06 pm) was focused with a Goebel mirror, and Cu-Kα_2 radiation was eliminated by the application of a Ni-absorber. The diffraction patterns were recorded and analysed with the Bruker AXS Diffrac-Suite.
Functionalized membranes, before and after sensing as well as respective samples of the respective MOFs were prepared in open-stage sample holders with a poly(methylmethacrylate) (PMMA) cupola and a Si-wafer platform. The diffraction data of the MMMs was collected using reflection geometry, whereas all diffraction data for the pure MOFs were collected in transmission geometry. Prior to investigation, the MOF-samples were ground in a mortar and transferred to Lindemann glass capillaries (ø = 0.5 mm).

SEM/EDX: Electron microscopy images of **2**@PSF were recorded with a Jeol JSM-6510LV QSEM Advanced Electron Microscope with a LaB_6 cathode at 5 – 20 keV. The microscope was equipped with a Bruker Xflash 410 silicon drift detector and the Bruker ESPRIT software for EDX analysis. The membrane cross-sections were prepared through freeze fracturing after immersion in liquid nitrogen and then coated with gold by a Jeol JFC 1200 fine coater (at an approximate current of 20 mA for 20–30 s).

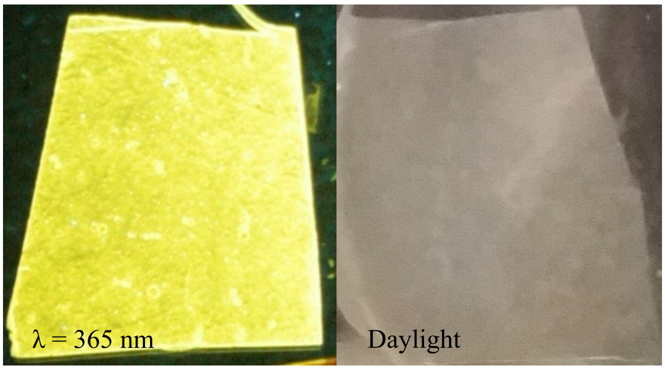

Figure. SI 1 MMMs **2**@PSF and their yellow emission excited at $\lambda_{exc.}$ = 365 nm (left) and under daylight (right).

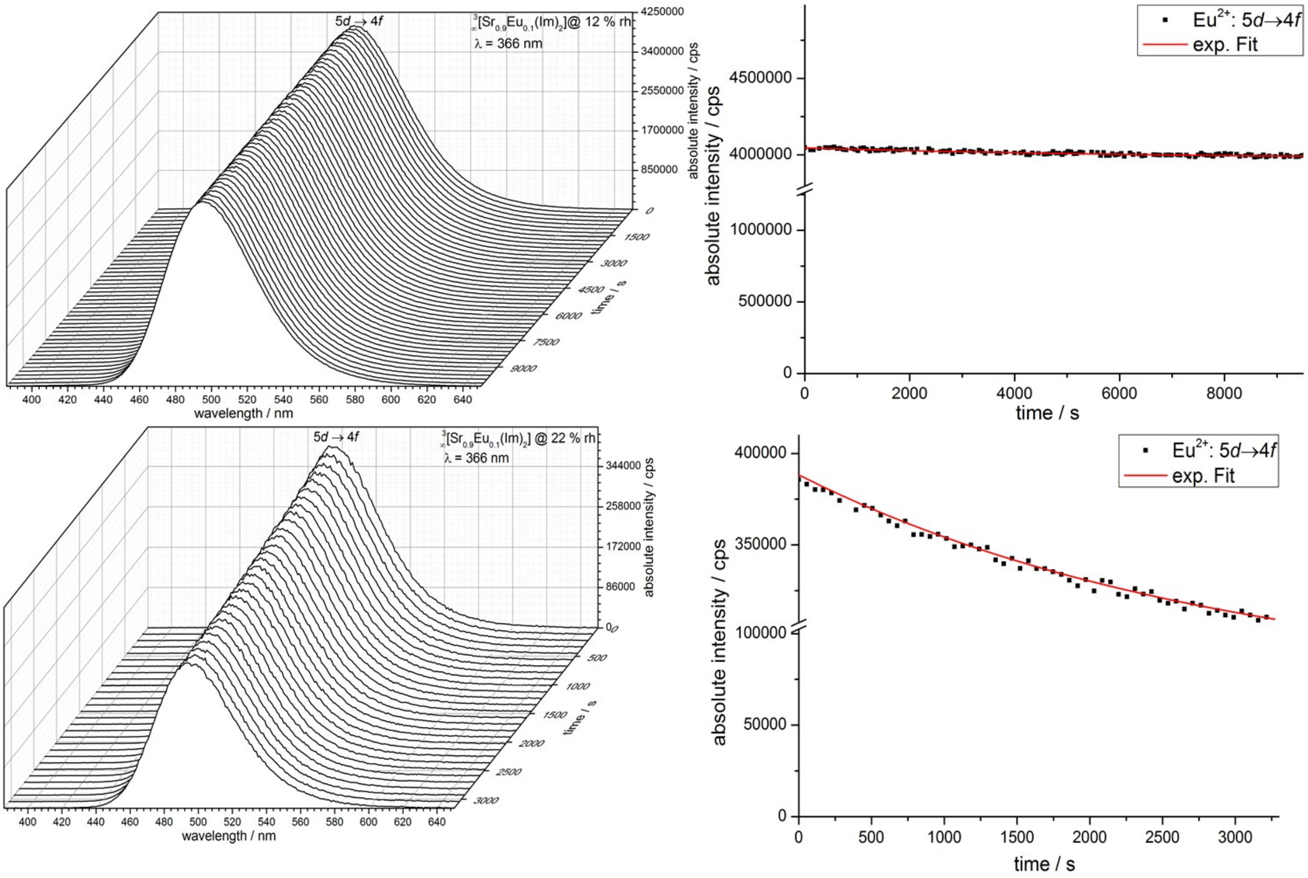

Figure SI 2 3D-photoluminescence emission spectra of the collected time-intensity related data and the corresponding emission maxima (left) and the exponential fit (right) of **2** at 12 % rh (top) and 22 % rh (bottom).

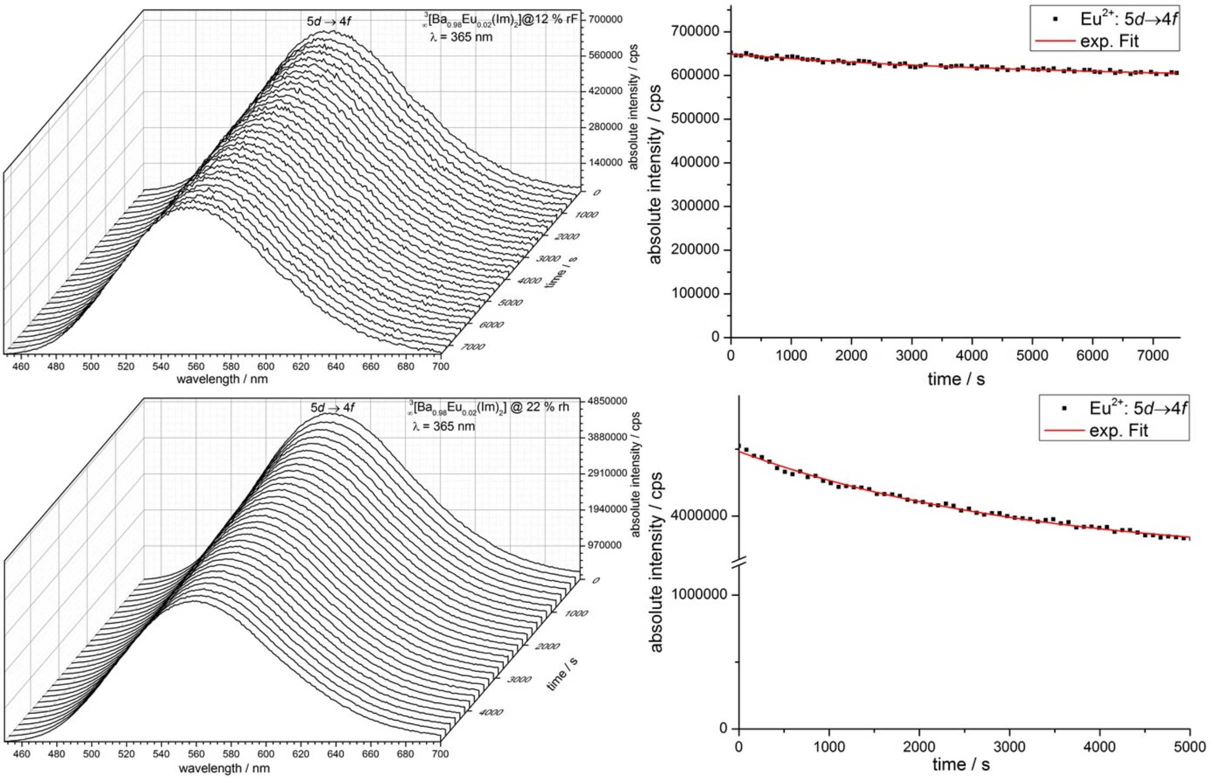

Figure SI 3 3D-photoluminescence emission spectra of the collected time-intensity related data and the corresponding emission maxima (left) and the exponential fit (right) of **1** at 12 % rh (top) and 22 % rh (bottom).

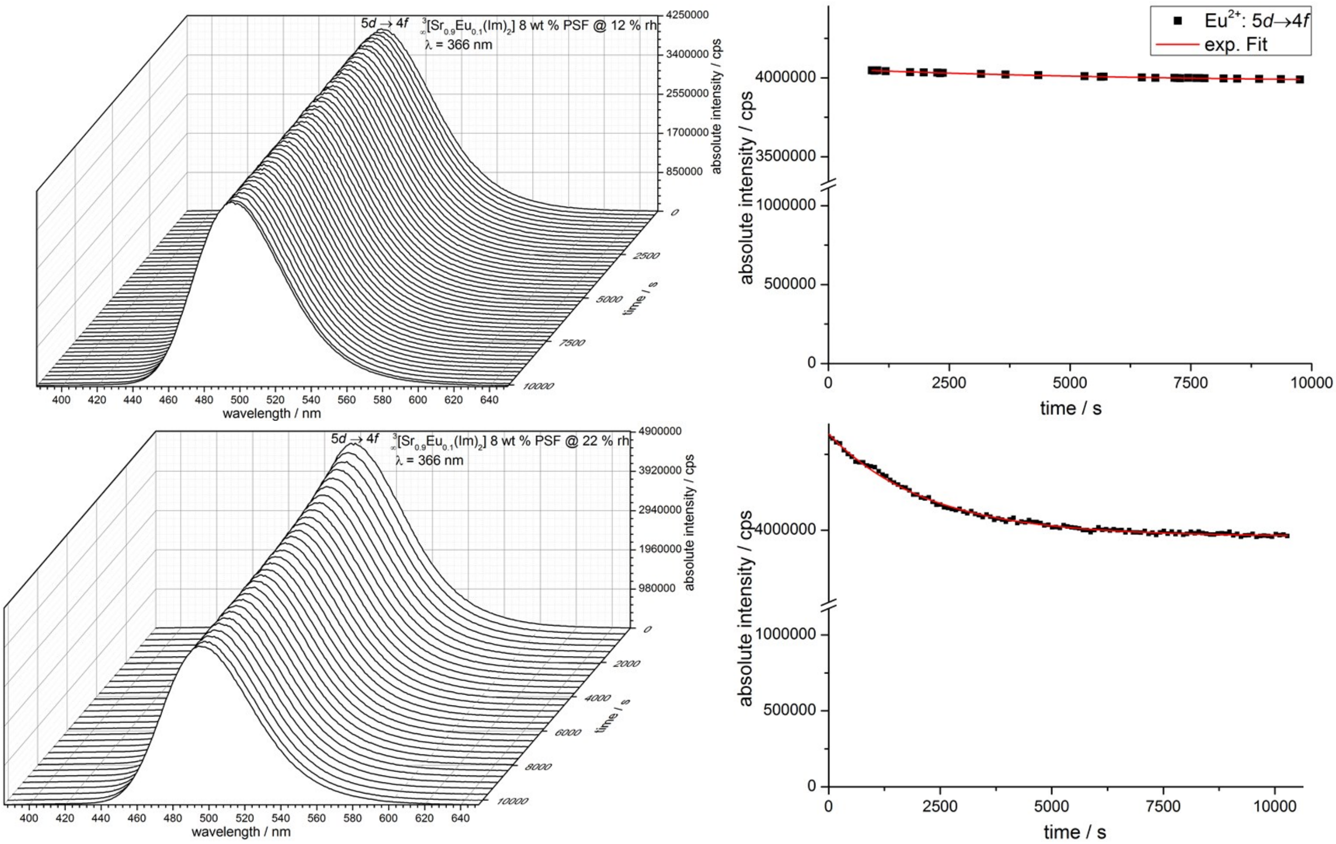

Figure SI 4 3D-photoluminescence emission spectra of the collected time-intensity related data and the corresponding emission maxima (left) and the exponential fit (right) of **2**@PSF at 12 % rh (top) and 22 % rh (bottom).

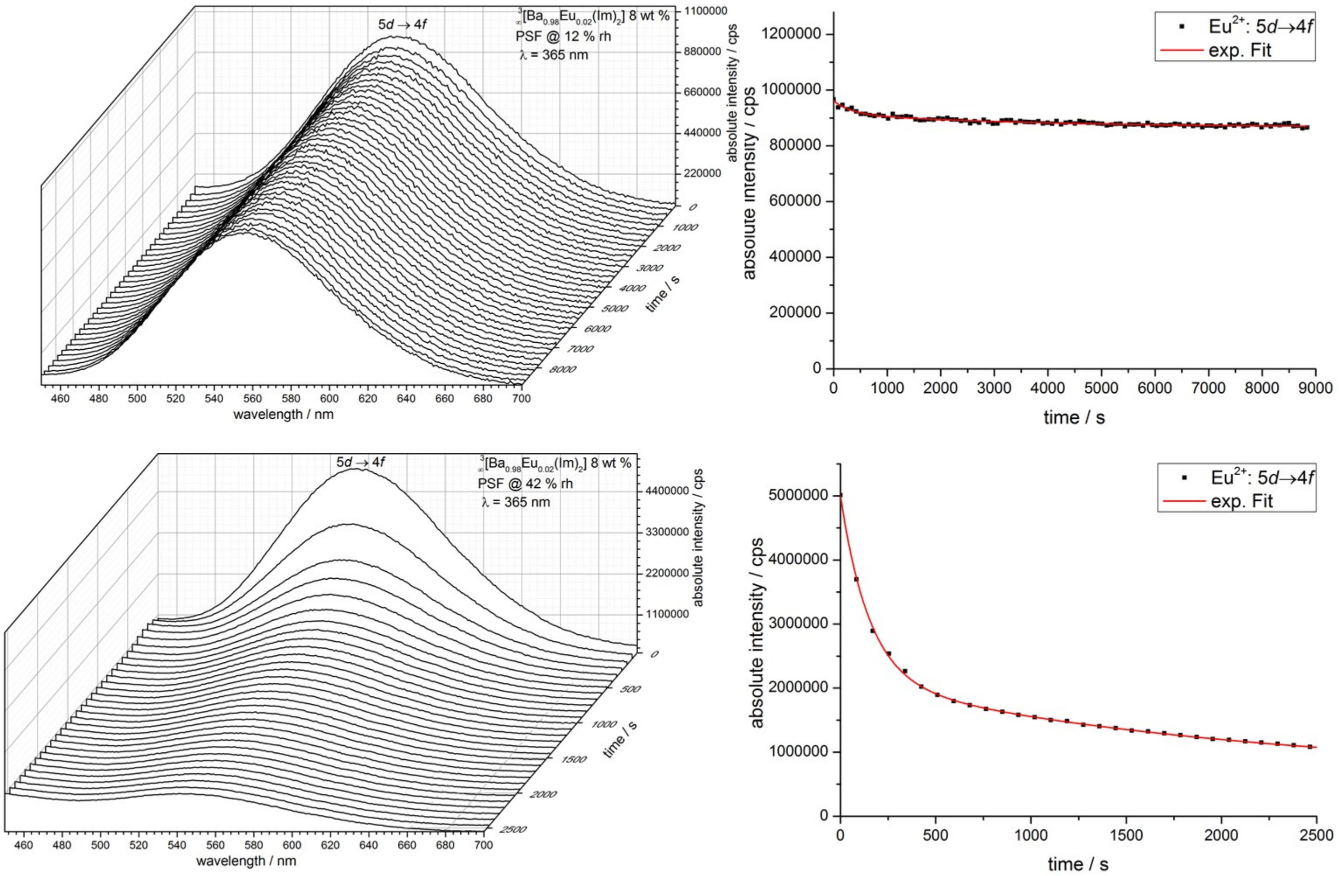

Figure SI 5 3D-photoluminescence emission spectra of the collected time-intensity related data and the corresponding emission maxima (left) and the exponential fit (right) of **1**@PSF at 12 % rh (top) and 42 % rh (bottom).

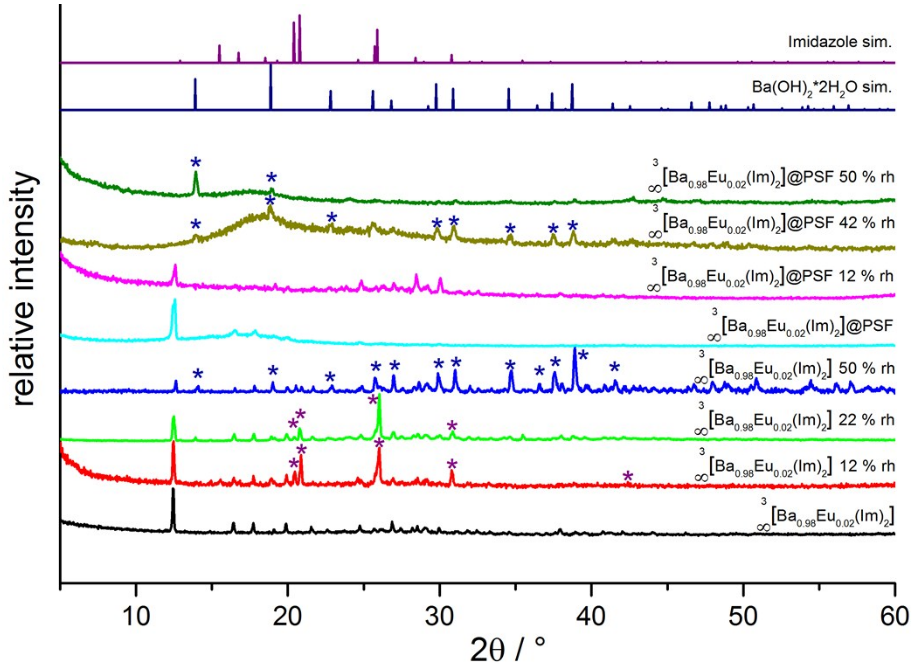

Figure SI 6 XRD powder patterns of **1** and **1**@PSF before and after sensing experiments. $Ba(OH)_2$•$2H_2O$ and imidazole included as reference. All new appearing reflections can be assigned to imidazole (2θ =20.45, 20.86, 26.02, 30.77, 42.39°) or $Ba(OH)_2$•$2H_2O$ (2θ = 14.08, 19.01, 22.88, 25.72, 26.96, 29.89, 31.03, 34,.69, 36.55, 37.58, 38.99, 41.53°).

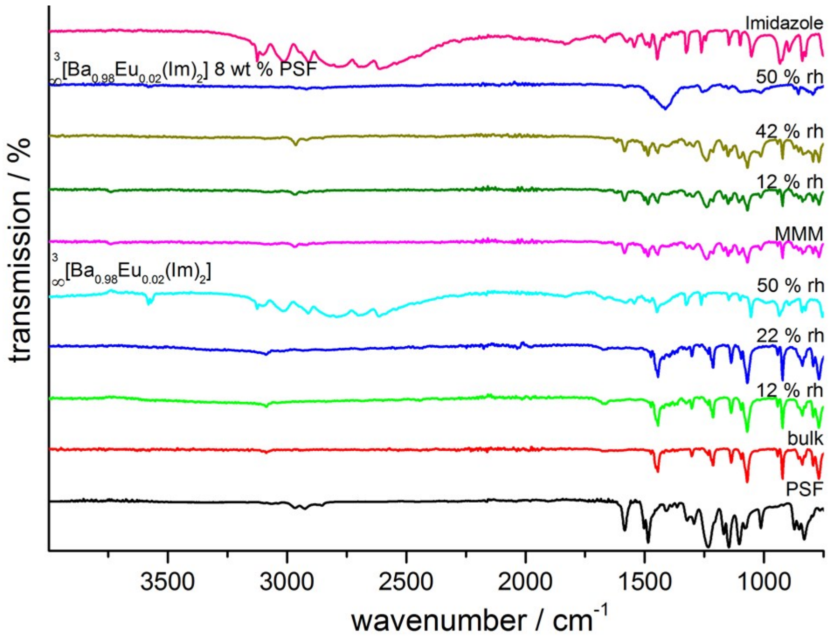

Figure SI 7 IR spectra of **1** and **1**@PSF before and subsequent to the sensing experiments. PSF and imidazole included as reference.

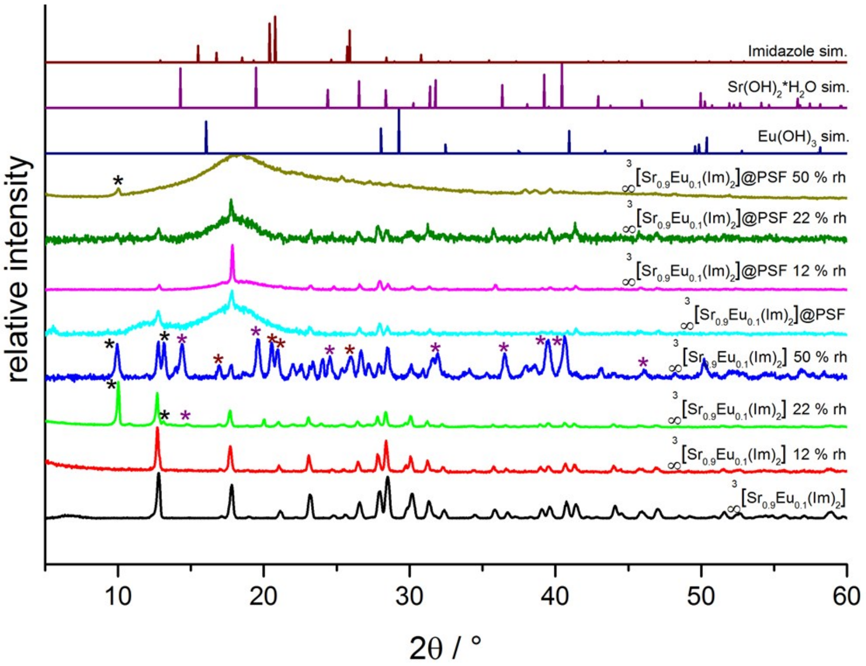

Figure SI 8 XRD powder patterns of **2** and **2**@PSF before and after sensing experiments. $Sr(OH)_2{\bullet}2H_2O$, $Eu(OH)_3$ and imidazole included as reference. Additional to imidazole (2θ = 16.94, 20.53, 20.99, 25.95°) and $Sr(OH)_2{\bullet}H_2O$ (2θ 14.39, 19.57, 24.52, 31.94, 36.52, 39.43, 40.62, 46.06°) an unidentified phase appears (2θ = 10.03, 10.76, 13.15, 14.71, 23.90°).

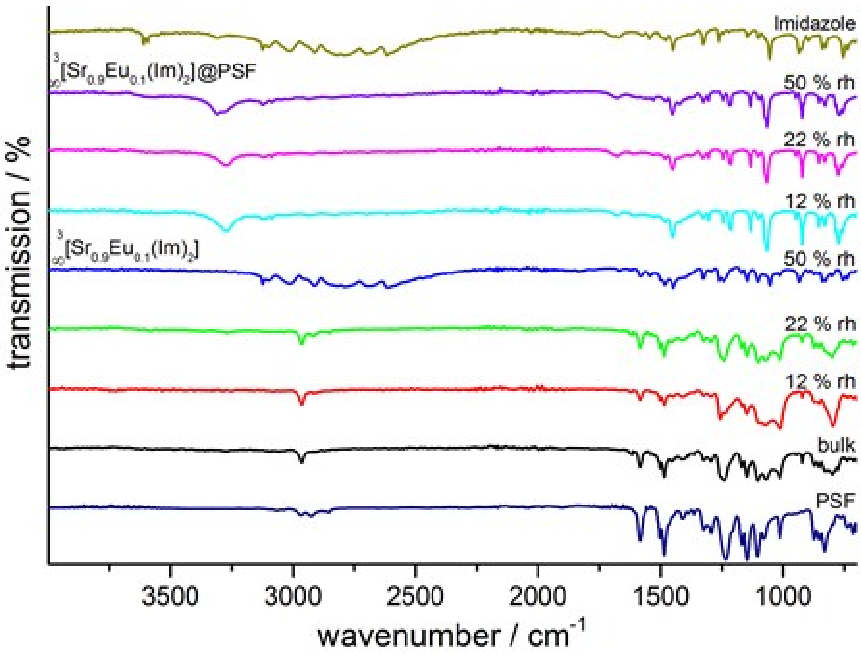

Figure SI 9 IR spectra of **2** and **2**@PSF before and subsequent to the sensing experiments. PSF and imidazole included as references.

Table SI 1 Elemental analysis of $_{\infty}[Ba_{0.98}Eu_{0.02}(Im)_2]$ **1** and $_{\infty}[Sr_{0.90}Eu_{0.10}(Im)_2]$ **2** before and after sensing of different relative humidity.

$_{\infty}$ $[Ba_{0.98}Eu_{0.02}(Im)_2]$	C%	H%	N%	aq. water
Bulk	26.52	2.95	20.61	0
12 % rh	26.13	3.21	18.75	0.5
22 % rh	25.18	3.08	18.46	1
50 % rh	22.70	3.44	16.89	2
$_{\infty}[Sr_{0.90}Eu_{0.10}(Im)_2]$	C%	H%	N%	aq. water
Bulk	32.26	2.84	24.24	0
12 % rh	31.53	2.92	23.02	0.5
22 % rh	28.30	4.03	20.56	1.5
50 % rh	22.05	5.88	14.68	5.5

Table SI 2 Parameters used for the Maxwell equation.

Chemical	Permeability $P_{m/f}$ [Barrer]	Density $\rho_{f/p}$ [g/cm³]	ω_f [mg]	ω_p [mg]	Φ_f
PSF	1.05	1.23	-	200	-
$_{\infty}[Ba_{0.98}Eu_{0.02}(Im)_2]$	0	2.296	18		0.046
$_{\infty}[Sr_{0.90}Eu_{0.10}(Im)_2]$	0	2.063	18		0.051

1 Barrer = 1 × 10^{-10} cm³ (STP)·cm/(cm²·s·cmHg) = 7.5005 × 10^{-18} m²·s^{-1}·Pa^{-1}

Equation used to calculate the volume fraction of the filler materials:

$$\Phi f = \frac{\omega f / \rho f}{\frac{\omega p}{\rho p} \times \frac{\omega f}{\rho f}}$$

Table SI 3 Gas permeation results for individual membranes

Membrane #	Permeability $P_{O2}(exp.)$ [Barrer] $_{\infty}[Ba_{0.98}Eu_{0.02}(Im)_2]$@PSF	Permeability $P_{O2}(exp.)$ [Barrer] $_{\infty}[Sr_{0.90}Eu_{0.10}(Im)_2]$@PSF	Permeability $P_{O2}(exp.)$ [Barrer] PSF
1	0.952	0.971	1.050
2	0.957	0.981	1.050
3	0.953	0.975	-
Avg.	0.954	0.976	1.050

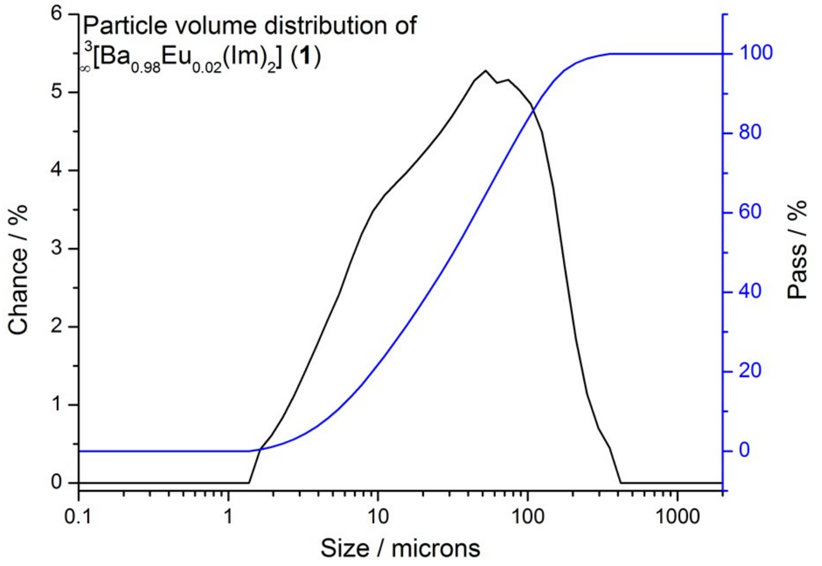

Figure SI 10 Particle volume distribution of **1** after ball milling for 150 s at 15 Hz.

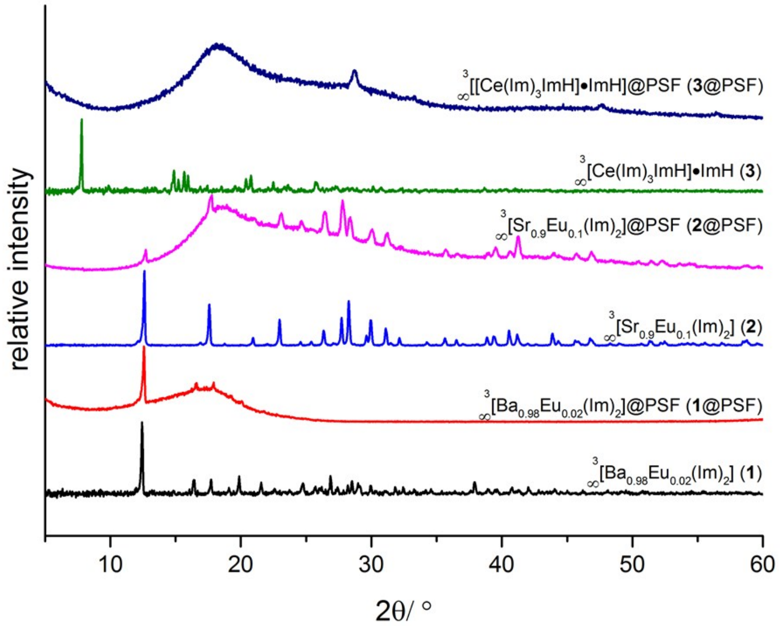

Figure SI 11 Comparison of the powder X-ray diffraction patterns of the MMMs **1**@PSF, **2**@PSF and **3**@PSF in comparison to the patterns of the bulk MOFs **1**, **2** and **3**.

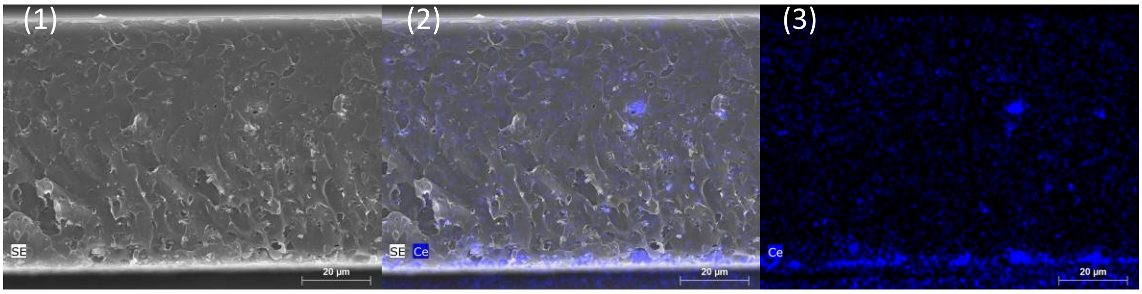

Figure SI 12 Cross-section SEM images of **3**@PSF. (1) shows the SEM image of **3**@PSF, (2) shows Ce distribution across the membrane overlaid with the SEM image, (3) shows the distribution of Ce. Minor sedimentation and aggregation are visible.

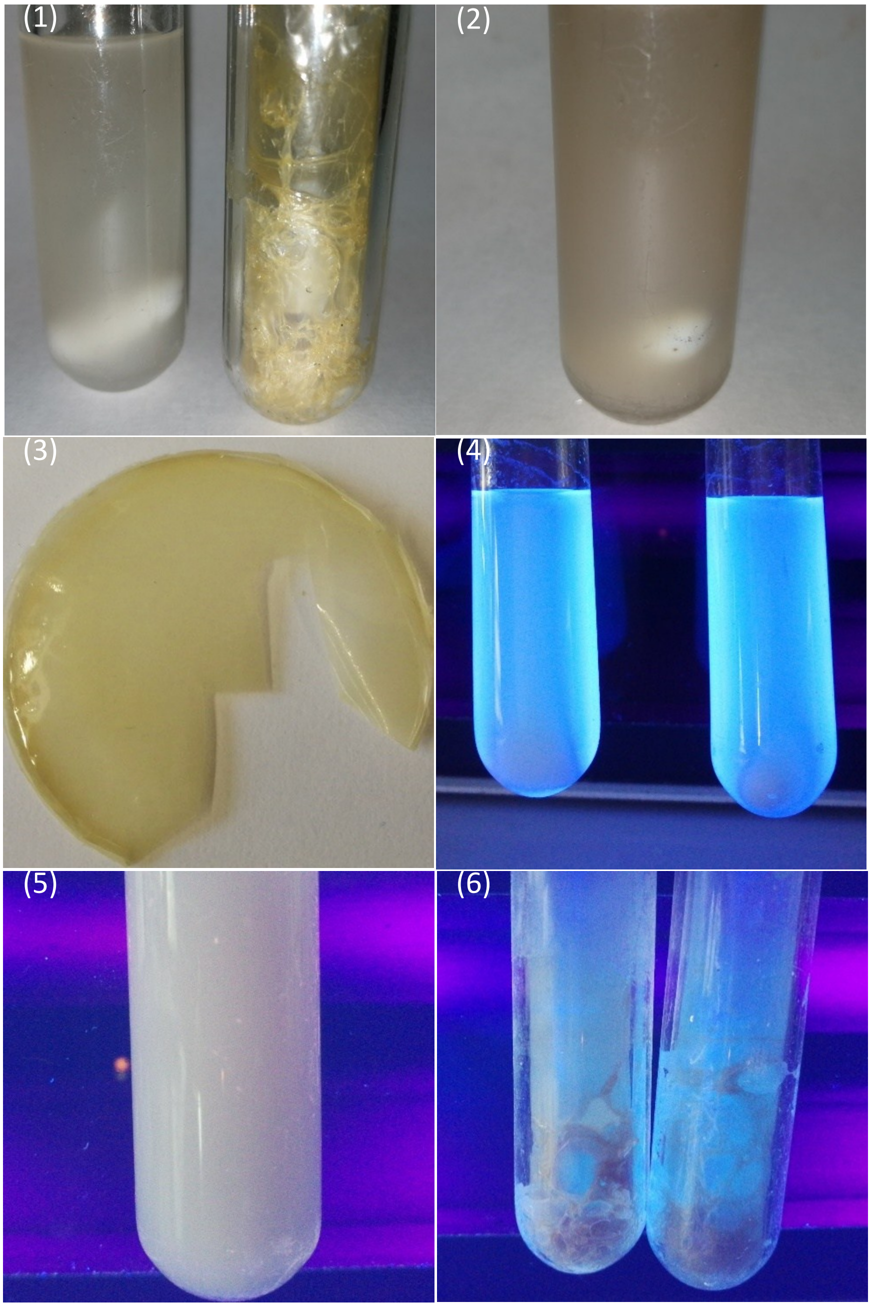

Figure SI 13 Different stages of **3**@PSF during membrane preparation. Part (1) shows a comparison between the grey MOF/polymer suspension in dichloromethane on the left and the dried MOF/polymer material on the right. A change from grey to yellow colour is visible. (2) shows the MOF/polymer suspension after stirring for 3 days. A colour change hinting at the decomposition of the MOF is also visible. In the suspension the MOF is still very dilute. As soon as the solvent in removed the yellow MOF colour becomes clearly visible. (3) shows a membrane of **3**@PSF. Parts of the membrane have been removed for further analyses. The yellow colour is clearly visible. (4) shows the luminescence of **3** while in the freshly prepared suspension in CH_2Cl_2 together with the polymer. (5) shows the complete loss of luminescence after stirring the suspension for 3 days under inert conditions. (6) shows the luminescence of the dried **3**@PSF. Reduction of the MOF luminescence and formation of a grey decomposition product is visible.